Desalination and Water Treatment
www.deswater.com

doi: 10.1080/19443994.2016.1156582

57 (2016) 25288–25300
November

Taylor & Francis
Taylor & Francis Group

Biosorption of malachite green from aqueous solution using brown marine macro algae *Sargassum swartzii*

M. Jerold, V. Sivasubramanian*

Department of Chemical Engineering, National Institute of Technology Calicut, Kozhikode 673 601, Kerala, India, email: jerold88@gmail.com (M. Jerold), +91 495 2285406; email: siva@nitc.ac.in (V. Sivasubramanian)

Received 16 October 2015; Accepted 30 January 2016

ABSTRACT

Batch biosorption experiments were carried out for the removal of malachite green (MG) from its aqueous solution using raw *Sargassum swartzii* biomass (RSSB) as biosorbent. The effect of various operating parameters was optimized for enhancing biosorption capacity. The biosorption capacity was found to increase with contact time and initial malachite green concentration. The biosorption of the dye was pH dependent and maximum uptake was observed at a pH of 10. The experimental data were analyzed using Langmuir, Freundlich, and Temkin equilibrium isotherm models. Langmuir isotherm ($R^2 = 0.98$) was found to fit the experimental data well. The biosorption kinetics of MG was found to follow pseudo-second-order kinetic model ($R^2 = 0.967$). The mechanistic study revealed that the biosorption of malachite onto RSSB was controlled by film diffusion. The characteristics of the RSSB biosorbent were studied using Fourier transform-infrared spectroscopy and scanning electron microscopy.

Keywords: Biosorption; Malachite green; Isotherm; Kinetics; Algae; Wastewater

1. Introduction

Nowadays, one of the key environmental issues faced by humanity is contamination of fresh water with several industrial contaminants [1]. Among the contaminants present in the industrial sewage, dyes are the most undesired pollutant, which are easily recognized by human eye. Furthermore, it significantly affects the photosynthetic activity in aquatic living system. Some of the dyes are degraded into toxic compounds which in turn have mutagenic or carcinogenic effects on living beings [2]. Several methods have been investigated for the removal of dyes from wastewater. Chemical precipitation is a common conventional treatment where a large quantity of chemical is necessary for the dye treatment which in turn generates a large volume of sludge [3,4]. Other treatment methods are ion exchange, activated carbon, filtration, electrolysis, and reverse osmosis which requires high capital investment and operational costs [5]. Thus, deliberately there is a need of alternative low-cost method that is more benign toward environment.

Therefore, much of the research works are focused on biological methods for the treatment of dye-bearing effluents [6–8], some of which are in the commercialization process. Among the biological method of dye decolorization, biosorption has been demonstrated to be an invariable potential method to replace the conventional method of dye removal. Biosorption is an emerging technology which is highly effective,

*Corresponding author.

economical, and widely used for the treatment of the textile effluent. It is the process based on the interaction between biomaterial–contaminant resulting in the sequestration of organic or inorganic pollutants [6]. Biosorption is the process of transfer of the dyes from the aqueous phase to a solid phase; thus reduces the degree of bioavailability in the environment [9]. The success of biosorption process depends on various factors such as right choice of biomaterials, renewable source, low cost, and their high sorption capacity [6] for the removal of contaminant. Biosorption is a finishing technology which completely removes the dye or reduces to very small levels [10]. Regeneration of biosorbent, greater efficiency, and ease of operation are the significant advantages of this method. Hence, these advantages together with their potent property have richly admired the researchers to exploit the various bio-resources as biosorbents for the wastewater treatment [11]. Number of biosorbents including bacteria [12], fungi [13], yeast [14], algae [15], and other agricultural waste [16], have indomitable affinity to bind with pollutants. The high biosorption capacity, easy availability, and low cost make the biosorption process more attractive. The sequestration of dye can be done by dead algal biomass. Particularly, macroalgae is supposed to have a predominant adsorptive behavior. Three main groups of macro algae are red algae, green algae, and brown algae. Among these, brown alga has peculiar properties like rich functional groups reusability for several cycles of adsorption. The algae collected from the ocean are recognized to have an impressive biosorption capacity [17]. *Sargassum*, a well-acknowledged species of brown algae are locally available in plenty of quantity. These algal species found mainly in the littoral zone of the marine environment are scattered in the brackish environment and known to exhibit as salt fenland fauna [18]. There are 13 different orders coming under the brown algal division Phaeophyta. Among those, Laminariales and Fucales are abundantly available in the marine environment. It is reported that they have lofty of biosorption potential [19]. Fucales are noteworthy and diversified order with a range of morphological diversity [19]. One of the most excellent genus of Fucales testified for the glorious biosorption is *Sargassum.* The biosorption performance is also due to the presence of two common moieties such as sulfate esters in the cellular polysaccharides and the presence of polyuronides [20]. Hence, the presence of functional groups in the uronic acids and availability of sulfated moieties could obviously serve as excellent ligand for the sorption of ions from the aqueous solution [21]. Therefore, the present investigation was undertaken to assess biosorption capacity of marine brown algae in the removal of cationic malachite green dye from aqueous solution. In this work, we have attempted to utilize the marine alga *Sargassum Swartzii* as biosorbent for the removal of malachite green from aqueous solution by batch process. The batch experiments were aimed to optimize the operational parameters. In the present study, the biosorption isotherm and kinetics for the sequestration of malachite green are also analyzed.

2. Materials and methods

2.1. Preparation of biosorbent

Raw *S. Swartzii* biomass (RSSB), collected from Mandapam, Tamil Nadu, India, was washed with large quantity of distilled water and sun-dried and subsequently dried in oven at 60°C for 24 h to remove the complete moisture. Dried samples were ground to an average particle size ranging from 0.5 to 1.0 mm and consequently used for the biosorption experiments without any further modification.

2.2. Dye solution and determination of dye concentration

Stock solution (1,000 mg/L) of dyes was dissolved in the distilled water and diluted to get the desired concentration of dyes. Fresh diluted dye solution was prepared for each experiment. The initial pH of the solution was adjusted with 1 mol/L of NaOH or HCl. Standard curves were developed through the measurement of absorbance at 617 nm at various concentration of MG by UV–visible spectrophotometer (2201; Systronics, India).

2.3. Characterization of biosorbent

The surface morphology of biosorbent and the involvement of functional groups are characterized using scanning electron microscopic (SEM) and Fourier transform-infrared spectroscopy (FTIR), respectively. Scanning electron micrograph shows the changes in the surface texture before and after biosorption of dye. Fourier transform infrared spectroscopy (FT-IR) spectra of RSSB before and after MG biosorption was collected in 4,000–500 cm^{-1} using FT-IR spectrophotometer (Nicolet Avatar 370, Thermo Scientific, India). Further, to know the percentage of elements C, H, N, and S in percentage, the RSSB was analyzed using C-H-N-S Analyzer (Vario EL III, Elementar, Germany).

2.4. Batch experimental program

Classical method of optimization is followed to determine the important process parameters such as

pH, contact time, biomass dosage, agitation rate, temperature, initial dye concentration for the removal of malachite green form aqueous solution. The experiment was conducted in a 250 mL Erlenmeyer flask with 100 mg/mL of dye solution. The flasks were agitated at 150 rpm for 3 h in a rotary shaker by adding 0.1 g of biosorbent. The initial pH of the solution was adjusted using 0.1 M HCl or NaOH in multiparameter portable meter (H19829; Hanna Instruments, USA). pH of the solution is monitored throughout the run and controlled using the same chemicals. After attaining equilibrium, the supernatant was withdrawn from the reaction mixture and the residual dye content was analyzed using double beam U-V spectrophotometer at a wavelength of 617 nm. In biosorption isotherm experiment, a predetermined quantity of biosorbent was added to the varied concentration of malachite green dye solution. Similarly, in batch kinetic experiment, the biomass was added to the dye solution of different initial concentration. At regular time intervals, samples were withdrawn and subjected to U-V analysis. The uptake of MG by RSSB was calculated using the mass balance:

$$q_e = \frac{(C_0 - C_e)V}{M} \quad (1)$$

where V is the solution volume (L), M is the mass of the biosorbent (g), and C_0 and C_e are the initial and equilibrium dye concentrations in the solution, respectively.

The rate of biosorption was calculated by conducting batch kinetic experiment in Erlenmeyer flask. Biomass was added to the solution at different concentration of MG dye and the samples were withdrawn at periodic time intervals and subsequently analyzed for the dye concentration. The dye uptake at time t, q_t (mg/g), was estimated using the mass balance:

$$q_t = \frac{(C_0 - C_t)V}{M} \quad (2)$$

2.5. Desorption and regeneration studies

The reusability of the biosorbent is the peculiar advantage of biosorption process. To assess the biosorption capacity of spent biosorbent, the dye loaded RSSB was subjected to the consecutive biosorption–desorption process. A maximum of three cycles of biosorption–desorption process was carried out. The spent RSSB was regenerated using 0.1 M HCl, where dye loaded RSSB was agitated at 150 rpm, 30°C in Erlenmeyer flask containing 100 mL of 0.1 M HCl for 60 min. The supernatant was subjected to the U-V analysis and the dye uptake was determined.

3. Results and discussion

3.1. Characterization of biosorbent

3.1.1. SEM analysis

The morphology of the RSSB is obtained using the scanning electron microscope to study surface characteristics of the biosorbent [22,23]. The scanning electron micrograph shows morphological changes in the surface texture before and after biosorption. Prior to the biosorption process, the biosorbent is rough and rigid as shown in (Fig. 1(a)) after the biosorption, the surface of the biosorbent seems to have a smooth morphological structure as shown in (Fig. 1(b)). This is due to the biosorption of dye onto the surface of the biomass [24]. Similar kinds of changes were noticed in the biosorption of dye by various biosorbents such as diatomaceous earth, *Ricinum communis*, and Tamarind fruit shell [25–27].

3.1.2. FT-IR analysis

The possible interaction between the biomass and dyes were investigated using the Fourier Transform Infrared Spectroscope. Fig. 2(a) and (b) shows the spectra before and after biosorption, respectively. The spectra indicate the absorption signals and the resultant functional groups present in the biomass. FTIR-spectra were obtained in the range of 4,000–500 cm^{-1}. The absorption bands 3,478, 1,622, 1,356, 1,012, and 839 cm^{-1} which indicated the presence of NH_2, C=O, C–O, C–O, and C–H groups, respectively (Fig. 2). Therefore, it is understood that the biomass consists of heterogeneous surface with various classes of active sites. Among these functional groups, amino groups play a vital role in the biosorption of MG. The other groups also have shown a less contribution in the binding of cationic MG dye. In fact, the relative importance of these functional groups depend on factors such as the quantity of sites, their accessibility, chemical state, and affinity between site and dye [28,29]. In most of the brown algae, carboxylic groups are generally richly present in the functional groups. About 70% of C=O groups are found in the dried algal biomass. Generally, the adsorption capacity is directly proportional to the presence of the active sites on the alginate which is ubiquitously present in the cell wall of brown algae both in the cell wall matrix and in the mucilage or intercellular material. The

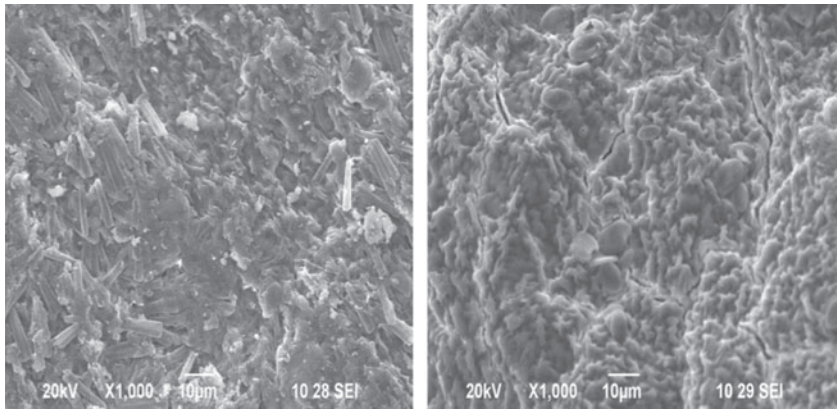

Fig. 1. Scanning electron microscopy images of *S. swartzii*: (a) before MG biosorption and (b) after MG biosorption.

polygulucronic acid can accommodate various monovalent and divalent ions. Also, they dimerizes in the presence of calcium ions. The hydroxyl groups also play an equal role in the biosorption of malachite green. At pH 10, the hydroxyl groups in the polysaccharides are negatively charged which enhances the sorption process.

3.1.3. EDAX analysis

The elemental composition of the biosorbent is obtained using EDAX analysis which provides the elemental information by means of X-ray emission. In the present investigation, RSSB was subjected to EDAX analysis before and after biosorption. EDAX

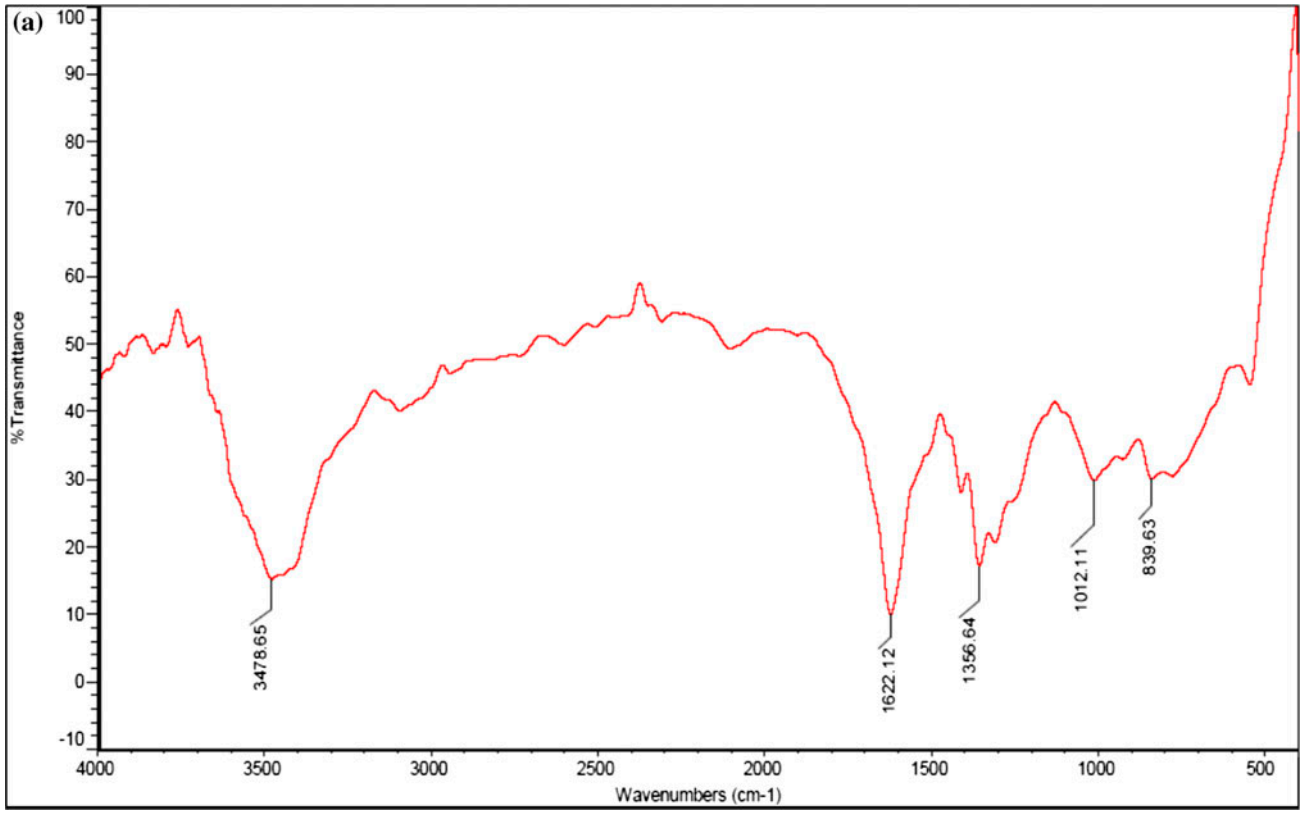

Fig. 2. (a) FT-IR spectra of RSSB and (b) FT-IR spectra of dye-loaded RSSB.

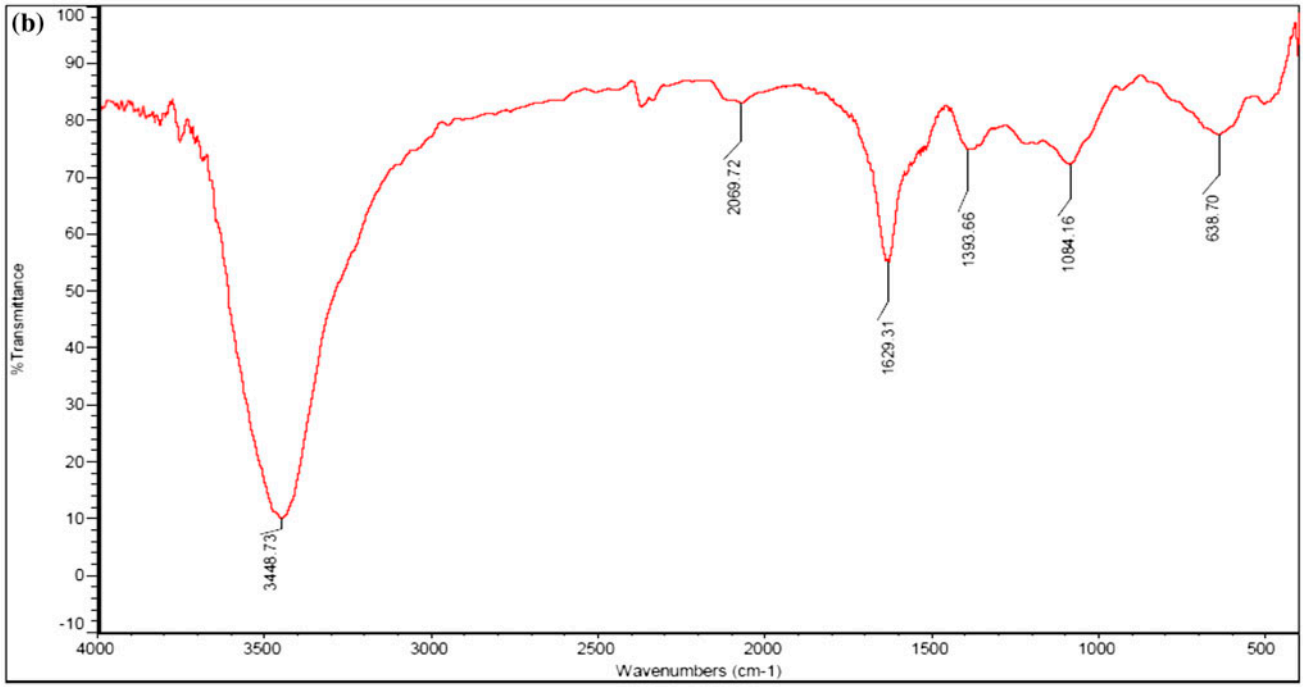

Fig. 2. (*Continued*).

spectrum of RSSB indicated the presence of the natural species such as O, Na, Mg, Al, Si, S, K, Ca, and Fe before MG biosorption (Fig. 3(a)). The response signals were due to the emission of X-ray from the biomolecules (proteins and polysaccharides) on the surface of the biomass, whereas after biosorption some of the elements like Na, Al, and Fe (Fig. 3(b)) disappeared which indicated the influence of the elements in the biosorption process. Thus, it revealed that ion-exchange mechanism is involved in the process of dye biosorption [30].

3.1.4. CHNS analysis

Based on the elemental composition, the percentage of carbon content in the RSSB is higher (Table 1). So, RSSB is a highly carbon-containing molecule and plays an important role in the biosorption of dye,

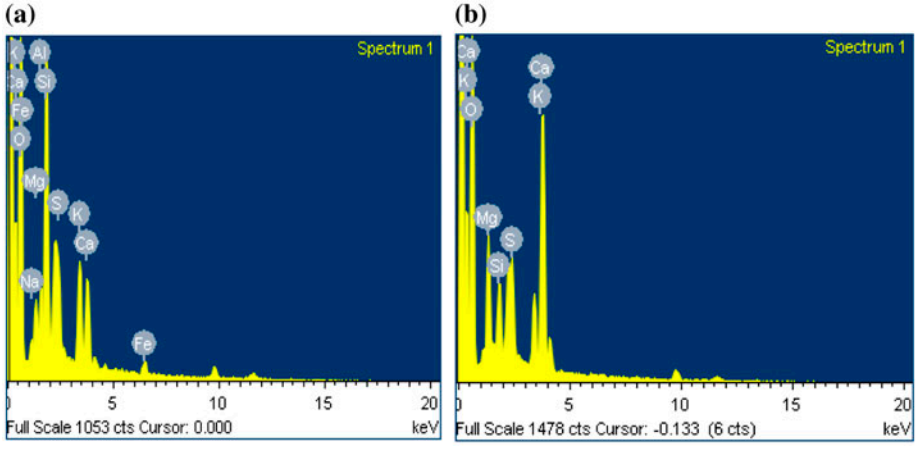

Fig. 3. EDAX spectrum of *S. swartzii*: (a) before MG biosorption and (b) after MG biosorption.

particularly the cellular polysaccharides and the presence of polyuronides [20].

3.2. Effect of pH

Initial experiments pertaining to the effect of equilibrium pH on dye removal revealed that alkaline conditions suit well for the maximum and effective dye removal. Thus at pH 10.0, there was maximum dye uptake of 59.33 mg/g as shown in Fig. 4. When the pH of the solution is decreased there is a reduction in the dye uptake. It is because at a higher pH the biomass surface gets negatively charged, which enhances sorption of positively charged cationic dye through electrostatic force of attraction and at lower pH, the protonation occur on the cell wall of the biomass (i.e.) formation of positive charged ions (H^+) which competes with cationic dye, therefore the sorption of dye is decreased [31,32]. More works have been done on biosorption of MG using various biosorbents. In all of these works, the analysis over a pH range of 4–10 showed that there is a threefold increase in decolorization.

3.3. Effect of biosorbent dosage

The effect of biosorbent dosage on the removal of MG by RSSB at C_o = 100 mg/L is shown in Fig. 5. It is observed that as the biosorbent concentration increased, there was a negative influence in the uptake of the dye. The decrease in MG uptake at higher adsorbent dose may be due to the competition of sorbate for the active sites available. This phenomena is due to the splitting effect of flux (concentration gradient) between the sorbent and sorbate [31]. However, percentage removal was increased due to rapid superficial biosorption at an increased biosorbent dosage and less solute concentration [33,34].

3.4. Effect of initial dye concentration and contact time

The effect of initial concentration on MG biosorption was investigated by varying the dye concentration between 20 and 100 mg/L. A plot of dye uptake q vs. time t at various initial dye concentrations is shown in Fig. 6. The uptake of the dye was increased with an increase in the initial dye concentration due to increase in the driving force. At initial stage, dye uptake was rapid on the external surface of the biosorbent followed by an internal diffusion which was the rate controlling step. This happened mainly due to larger number of active sites available in the biosorbent during the initial stage. Later, repulsion exerted and the active sites were occupied, thus there was a delay in the equilibrium attainment. Therefore, the initial dye concentration comprising of larger ions competing for the vacant active sites on the biosorbent resulted in higher biosorption capacity which in turn increased the dye uptake rate.

Table 1
CHNS analysis of RSSB

Element	Percentage (%)
C	30.11
H	4.66
N	0.96
S	0.45

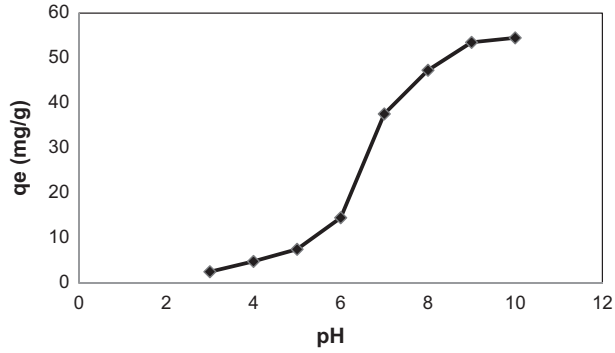

Fig. 4. Effect of pH (V: 100 mL; C_0: 100 mg/L; M: 0.1 g; Temp. 30°C).

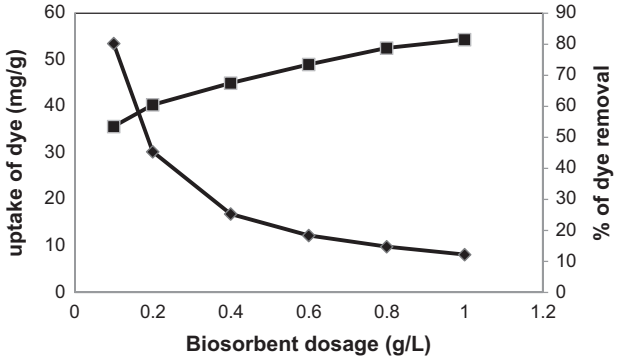

Fig. 5. Effect of RSSB dosage (V: 100 mL; C_0: 100 mg/L; M: 0.1 g; Temp. 30°C).

3.5. Effect of agitation

Agitation influences the biosorption of MG. Hence, the effect of agitation was studied by varying the agitation speed from 50 to 200 rpm using 1 g/L of biosorbent and 100 mL of 100 mg/L of dye solution at

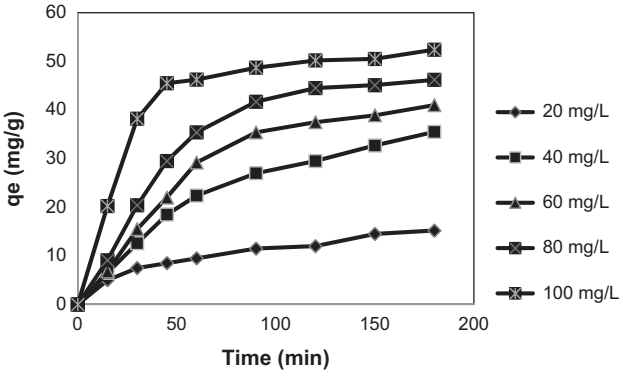

Fig. 6. Effect of initial dye concentration (V: 100 mL; C_0: 100 mg/L; M: 0.1 g; Temp. 30˚C).

pH 10.0. At lower agitation (50 rpm), the uptake of the dye was recorded as 21.5 mg/g. But when the rate of agitation was increased from 50 to 150 rpm there was an appreciable increase in the uptake of the dye from 21.5 to 56.2 mg/g, respectively, as shown in Fig. 7. It is basically due to the enhancement of turbulence, the rate of diffusion of dye molecules from bulk liquid to the liquid boundary layer surrounding the particle becomes higher and decrease of thickness of the liquid boundary layer. External sorption kinetic control plays a significant role [35]. Further, increase in agitation leads to the down regulation of dye uptake. This is probably due to the collision of the sorbate molecules which is attributed to an increase in desorption tendency of dye molecules. Higher mixing results in higher shear force which causes bond breakage between MG and biosorbent [36].

3.6. Biosorption isotherms

In the design and analysis of biosorption process, isotherms bestow a piece of information underlying biosorption mechanism as well as the surface properties and affinity of the biosorbent. Generally, the biosorption isotherms are the computation of the concentration of adsorbate in the bulk phase and interface of biosorbent at equilibrium [37]. Three different mathematical isotherm models (Langmuir, Freundlich, and Temkin) were used for validating the experimental results. Langmuir is the most widely used model for the description of adsorption process [38]. It has two assumptions (a) the adsorbed molecules have no further interaction between the adsorbate and (b) the formation of saturated monolayer of solute molecules on the surface of the adsorbent. The linearized form of the Langmuir isotherm equation is as follows:

$$\frac{1}{q_e} = \frac{1}{K_L q_{max}} \left(\frac{1}{C_e}\right) + \frac{1}{q_{max}} \tag{3}$$

where q_e (mg/g) is the amount of dye adsorbed per unit mass of the biosorbent and C_e (mg/L) is the amount of adsorbed dye per unit mass of sorbent and unadsorbed dye concentration in solution at equilibrium. q_{max} maximum uptake of dye per unit mass of the biosorbent in order to form monolayer on the surface of algal biomass at an equilibrium concentration, and K_L is a binding affinity constant related to the affinity toward the sorbate (L/mg).

The plot of specific adsorption ($1/q_e$) against the equilibrium concentration ($1/C_e$) (Fig. 8) is linear. So it is concluded that particular adsorption system obeys the Langmuir model. The slope and intercept of the plot reciprocates the Langmuir constants q_{max} and K_L, respectively, and are tabulated in Table 2.

The Langmuir separation factor R_L is a dimensionless constant which is the important characteristic of

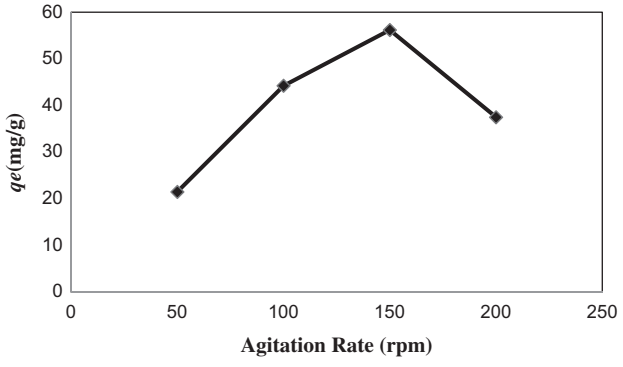

Fig. 7. Effect of agitation (V: 100 mL; C_0: 100 mg/L; M: 0.1 g; Temp. 30˚C).

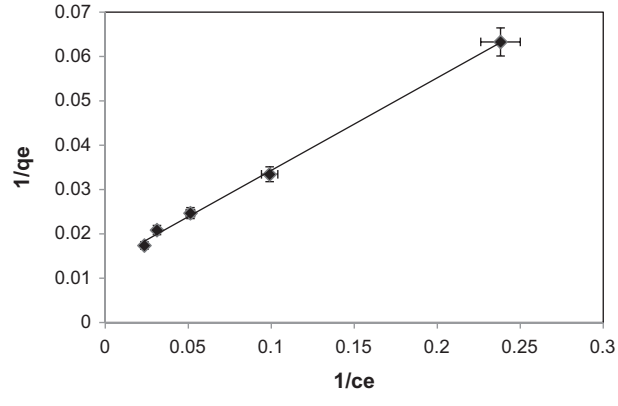

Fig. 8. Langmuir isotherm plot for MG sorption onto RSSB at 30˚C.

Table 2
Langmuir, Freundlich, and Temkin isotherm model constants and correlation coefficients for adsorption of MG onto RSSB

Isotherm	Parameters
Langmuir	
q_{max} (mg/g	76.92
K_L (L/mg)	0.0062
R^2	0.998
Freundlich	
K_F (mg/g)	7.830
n	1.862
R^2	0.980
Temkin	
A (L/g)	1.750
B	17.20
R^2	0.987

Langmuir isotherm. Langmuir isotherm is presented in the following equation:

$$R_L = \frac{1}{(1 + K_L C_0)} \quad (4)$$

where C_0 is the maximum initial concentration of adsorbate (mg/L), and K_L (L/mg) is Langmuir constant.

The separation factor R_L can be described on the shape of isotherm either unfavorable ($R_L > 1$), linear ($R_L = 1$), favorable ($0 < R_L < 1$), or irreversible ($R_L = 0$). In the case of favorable isotherm, the R_L values are between 0 and 1. In the present study, biosorption of MG onto RSSB, the R_L value was found to be 0.617 (Table 3). Therefore, the adsorption is favorable.

Freundlich isotherm model describes the biosorption in a heterogeneous system [39]. It is being noted that at pH 10 both K_F and n (Freundlich constants) reached their maximum values. Thereby, there is an inclination in the biosorption capacity as well as the affinity between biomass and dye [40]. The linearized Freundlich equation is:

$$\ln q_e = \ln K_F + \frac{1}{n} \ln C_e \quad (5)$$

where K_F (mg/g) is the biosorption capacity of the sorbent and n represents the biosorption favorability. The purpose of Freundlich isotherm is that the deducible constants are integrated in these isotherms. The degree of exponent, $1/n$ describes the favorability of biosorption process. Suppose, $n > 1$ then it naturally reflects that adsorption is favorable [41]. A plot (Fig. 9) of $\ln(q_e)$ against $\ln(C_e)$ derived from linearized Freundlich equation is used to determine the constant values K_F and $1/n$.

Table 3
Langmuir separation factor for RSSB

Initial MG dye concentration (mg/L)	R_L
20	0.889
40	0.801
60	0.728
80	0.668
100	0.617

The Temkin isotherm model takes into account the interactions between adsorbate and adsorbent species. Temkin isotherm assumes that the heat of adsorption decreases linearly on a surface [42] and the molecules adsorbed over the surface are epitomized with consistent binding energies up to a notable maximum value. Consequently, Temkin and Pyzhev suggested that due to the effect of indirect interaction of sorbate molecules, there is a significant reduction in the heat of adsorption of the sorbate on the surface of the adsorbent. The linearized Temkin isotherm is presented as follows:

$$q_e = B \ln A + B \ln C_e \quad (6)$$

where $B = RT/b$, b is the Temkin constant related to heat of sorption (J/mol); A is the Temkin isotherm constant (L/g), R the universal gas constant (8.314 J/mol K), and T the absolute temperature (K).

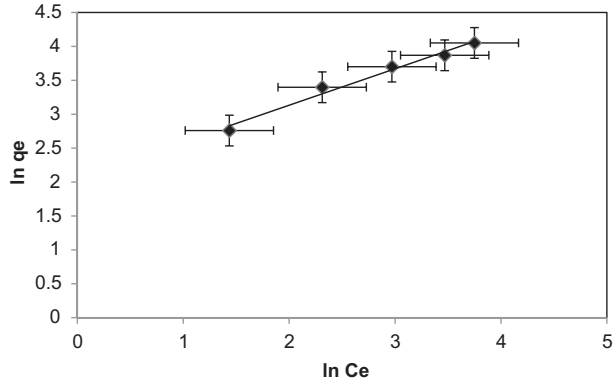

Fig. 9. Freundlich isotherm for MG sorption onto RSSB at 30°C.

Therefore, by plotting q_e vs. ln C_e the constants A and B are determined as shown in Fig. 10. The constants A and B are listed in Table 2.

The experimental data were analyzed using Langmuir, Freundlich, and Temkin isotherms. From the analysis, the experimental data of MG biosorption onto RSSB fitted well with Langmuir isotherm than with Freundlich and Temkin isotherms as in Table 2. The results indicated the homogeneous nature of biosorbent by the monolayer coverage on surface between the sorbed molecules. The maximum Langmuir biosorption capacity was found to be 76.92 mg/g. Table 4 compares the bisorption capacity of different types of adsorbent used for removal of MG. The most important parameter to compare is the q_{max} value since it is a measure of adsorption capacity of the biosorbent. The value of q_{max} in this study is larger than those in most of previous works. This suggests that MG could be easily adsorbed on surface of RSSB.

3.7. Biosorption kinetics

Lagergren pseudo-first-order model [51] is presented as follows:

$$\log(q_e - q_t) = \frac{\log q_e - k_1 t}{2.303} \tag{7}$$

A linear plot of $\log(q_e - q_t)$ vs. time gives the rate constant of the reaction. The linearity of the plot with good coefficient of determination indicated Lagergren pseudo-first-order model is appropriate to the biosorption of MG onto RSSB [52]. In the present investigation, respective constants of the first-order kinetics (k_1) and q_e are evaluated from the Lagergren's model and presented along with their corresponding R^2 values in Table 4.

The linearized pseudo-second-order kinetics can be expressed as [53]:

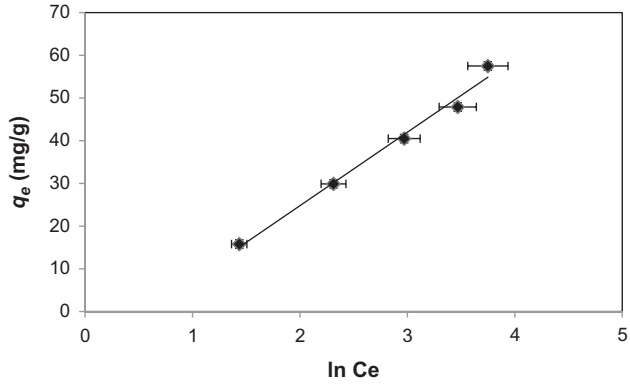

Fig. 10. Temkin isotherm for MG sorption onto RSSB at 30°C.

$$\frac{t}{q_t} = \frac{1}{k_2 q_e^2} + \frac{t}{q_e} \tag{8}$$

where (q_e) equilibrium adsorption capacity and k_2 (g/mg h), the second-order constant can be determined from the plot of t/q_t vs. t. The values of k_2 and q_e are computed from the model and are presented along with their respective correlation coefficients in the Table 5. In pseudo-second-order model, it is assumed that the sorption capacity is proportional to the number of active sites occupied on the sorbent, hence the kinetic rate law [53] can be written as:

$$\frac{t}{q_t} = \frac{1}{h} + t\left(\frac{1}{q_e}\right) \tag{9}$$

where $h = k_2/q_e^2$. The values ($1/h$) and q_e can be determined from the intercept and slope, respectively, from a linear plot of t/q_t and time.

From Table 5, it is observed that the experimental data fitted well with pseudo-second-order model than

Table 4
Comparison of biosorption capacities of various adsorbents for Malachite Green

Adsorbents	q_{max} (mg/g)	T (°C)	Refs.
RSSB	76.92	30	This study
Turbinaria conoides	66.6	30	[43]
Pleurotus ostreatus	32.33	25	[44]
Arundo donax root carbon	8.70	30	[45]
Bentonite clay	7.72	35	[46]
Tamarind fruit shell	1.95	30	[47]
Immobilized *S. Cerevisae*	17.0	35	[48]
Cellulose powder	2.42	25	[49]
Rubber wood sawdust	25.8–36.3	–	[50]

Table 5
Kinetic parameters for the MG biosorption onto RSSB

Kinetic model	Parameters
Pseudo-first-order	
K_1 (1/min)	0.018
R^2	0.917
Pseudo-second-order	
K_2 (g/mg min)	0.001
R^2	0.988
h (mg/g min)	1.79×10^{-5}
$q_{e,cal}$ (mg/g) 90.90	55.56
Intraparticle diffusion	
K_{id} (mg/g $h^{1/2}$)	3.744
C	10.02
R^2	0.824
Boyd Kinetic model	
B	0.021
D_i	4.185×10^{-5}
R^2	0.898

with pseudo-first-order model. Hence, the pseudo-second-order model better represented the adsorption kinetics.

3.8. Mechanism of biosorption

The two familiar kinetic models such as pseudo-first-order model and pseudo-second-order model have failed to explain the mechanism and rate-limiting steps in the biosorption process. Hence, the study was extended to deal with Weber and Morris intra-particle diffusion model [54] and Boyd kinetic plot. The transfer of solute from solid to liquid biosorption process is characterized by the film diffusion and/or particle diffusion [55]. The following steps occur repeatedly during the biosorption of MG onto RSSB (film diffusion):

(1) Transfer of sorbate (MG) from the bulk solution to the exterior solid (RSSB) surface (film diffusion).
(2) Diffusion of MG into the pores of RSSB—trivial amount of biosorption in the exterior surface of RSSB is neglected (particle diffusion).
(3) A considerable amount of biosorption of MG on the interior surface of RSSB [29].

To study the adsorption mechanism, the kinetic data of adsorption are fitted into intra-particle diffusion equation and Boyd kinetic equation.

3.8.1. Intra-particle diffusion

Intra-particle diffusion model empirically noted that most common functional relationship to describe the mechanism of adsorption process. Weber's intra-particle diffusion equation [54] illustrates the mechanism and the rate controlling steps which causes the adsorption kinetics. The experimental data are fitted with the Weber's intraparticle diffusion. The diffusion mechanism is obtained by elucidating the kinetics with the intraparticle diffusion model. The model is expressed as:

$$q_t = K_{id} t^{1/2} + C \tag{10}$$

where C and k_{id} are intercept and intraparticle diffusion rate constant (mg/g $h^{1/2}$), respectively, the values can be evaluated from the plot q_t vs. $t_{1/2}$ [54] and listed in Table 5. The boundary layer effect explains the rate controlling steps. The intercept of the plot represents the boundary layer effect. Larger the intercept, greater the contribution of the surface sorption in the rate controlling step. If the plot q_t vs. $t_{1/2}$ is linear and the regression of the line passes through the origin, one can say that rate-limiting step is governed by intraparticle diffusion. However, in the present study at various concentrations, an absolute linearity was not obtained, and hence they did not pass through the origin ($R^2 < 0.93$). This clearly illustrates that the intra-particle diffusion was not only the sole rate controlling step. Also, it can be seen from the small value of the intra-particle diffusion constant that the boundary layer has less significant effect on the diffusion mechanism of dye uptake with the algal biosorbent.

3.8.2. Boyd kinetic model

The slow biosorption of MG on to RSSB is validated by subjecting the experimental data to Boyd kinetic model analysis. The Boyd kinetic equation is:

$$F = \frac{q_t}{q_e} = 1 - \frac{6}{\pi^2} e^{(-Bt)} \tag{11}$$

Eq. (11) rearranged and written as [31]:

$$Bt = -0.4977 - \ln(1 - F) \tag{12}$$

where q_e is the equilibrium biosorption capacity (mg/g), q_t is the biosorption capacity at any time (mg/g), F is the fraction of MG adsorbed at any time (t), and Bt is a function of F. The linear plot of "Bt vs.

Table 6
Thermodynamic parameters of RSSB at different temperature

Temp. (K)	K_C	ΔG° (kJ/mol)	ΔH° (kJ/mol)	ΔS° (kJ/mol/K)
303	1.164	−383.69	37604.22	125.29
313	1.816	−1,554.09		
323	2.968	−2,922.02		
333	4.405	−4,105.80		

t'' indicates that particle diffusion is the slowest step in the biosorption of MG on to RSSB. In the present study, an absolute linearity was not obtained at various concentrations hence they did not pass through the origin ($R^2 < 0.93$) which indicated that film diffusion controls the biosorption of MG onto RSSB. The constant values are obtained from the plot and tabulated in Table 5. The biosorption diffusion coefficient D_i (m^2/s) is calculated using the following equation:

$$B = \frac{\pi^2 D_i}{r^2} \tag{13}$$

where D_i is the effective diffusion coefficient and r is the radius of RSSB.

3.9. Thermodynamic studies

Biosorption is a temperature-dependent process. Thermodynamic analysis of equilibrium sorption data assist to determine the spontaneity and heat exchange of malachite green biosorption onto the RSSB as well as gives a brief knowledge on the thermodynamic parameters such as change in free energy (ΔG), enthalpy (ΔH), and entropy (ΔS). The Gibbs free energy change for biosorption of MG onto RSSB is estimated using the following expression:

$$\Delta G^\circ = -RT \ln K_c \tag{14}$$

Vant Hoff's equation gives a general relation between the standard enthalpy change and standard entropy change which is expressed as follows:

$$\ln K_c = \frac{-\Delta H^\circ}{RT} + \frac{\Delta S^\circ}{R} \tag{15}$$

where K_c is equilibrium constant for sorption, R gas constant, T temperature (K). The value of ΔH° was calculated from the slope of the linear regression of $\ln K_c$ vs. $1/T$. The K_c value was determined by the relation given below:

$$K_c = \frac{q_e}{C_e} \tag{16}$$

where q_e denotes the quantity of MG adsorbed on RSSB at equilibrium (mg/L), C_e is the malachite green in solution at equilibrium concentration (mg/L). Table 6 illustrates the thermodynamic parameters that were calculated by above equations. ΔG° gives a hint about the type of adsorption. In the present investigation, negative ΔG° value indicates the feasibility and spontaneous nature for the biosorption of malachite green. Hence, it confirms the affinity of RSSB for MG sorption. Another thermodynamic parameter, ΔH° was found to be positive, which indicates the endothermic nature of the biosorption processes. In addition, the positive standard entropy reveals that there is an increase in randomness at the solid–liquid interface during the sorption of MG onto the surface of RSSB.

3.10. Desorption and regeneration studies

Regeneration and recycle of the spent biosorbent are novel features of the biosorption process which can be executed by means of the desorption process. RSSB is effectively utilized for the biosorption of MG. From this study, it was observed that the biosorption capacity of RSSB tends to reduce after each cycle of operation viz 57.2, 49.5, and 35.67 mg/g, respectively. Thus, it is understood that RSSB has good biosorption capacity due to the presence of thick thallus [17]. The acid treatment eliminates the impurities and other sorbate molecules and creates vacancy of binding sites in the biomass.

4. Conclusion

RSSB is found to be an effective biosorbent for the sequestration of dye bearing wastewater. RSSB is a low-cost biosorbent which is effectively utilized for the removal of MG from aqueous solution. The SEM images of RSSB before and after biosorption have revealed the effective biosorption of MG. The optimization of physical parameters were carried out by

varying pH, biosorbent dosage, initial dye concentration, agitation rate, contact time, and temperature for the maximum removal of MG. Biosorption Isotherm was analyzed by Langmuir, Freundlich, and Temkin models for the experimental data. Of which, Langmuir model fits well with the experimental data and the Langmuir monolayer biosorption capacity is found to be 76.92 mg/g. The biosorption kinetics was better to be explained by pseudo-second-order rather than the pseudo-first-order. In addition, Boyd kinetic study has explained the mechanism behind the biosorption of MG and it revealed that film diffusion controlled the biosorption process. Desorption and regeneration studies have showed that RSSB has immense property of reusability with minor decrease in biosorption capacity. In a nutshell, RSSB is a most promising biosorbent which can be used for the treatment of dye bearing wastewater.

References

[1] R.P. Schwarzenbach, B.I. Escher, K. Fenner, T.B. Hofstetter, C.A. Johnson, U. von Gunten, B. Wehrli, The challenge of micropollutants in aquatic systems, Science 313 (2006) 1072–1077.

[2] C. O'Neill, F.R. Hawkes, D.L. Hawkes, N.D. Lourenço, H.M. Pinheiro, W. Delée, Colour in textile effluents—Sources, measurement, discharge consents and simulation: A review, J. Chem. Technol. Biotechnol. 74 (1999) 1009–1018.

[3] P. Nigam, I.M. Banat, D. Singh, R. Marchant, Microbial process for the decolorization of textile effluent containing azo, diazo and reactive dyes, Process Biochem. 31 (1996) 435–442.

[4] H. Eccles, Removal of heavy metals from effluent streams—Why select a biological process? Int. Biodeterior. Biodegrad. 35 (1995) 5–16.

[5] G. Tiravanti, D. Petruzzelli, R. Passino, Pretreatment of tannery wastewaters by an ion exchange process for Cr(III) removal and recovery, Water Sci. Technol. 36 (1997) 197–207.

[6] P.J. Lu, H.C. Lin, W.T. Yu, J.M. Chern, Chemical regeneration of activated carbon used for dye adsorption, J. Taiwan Inst. Chem. Eng. 42 (2011) 305–311.

[7] T. Robinson, G. McMullan, R. Marchant, P. Nigam, Remediation of dyes in textile effluent: A critical review on current treatment technologies with a proposed alternative, Bioresour. Technol. 77 (2001) 247–255.

[8] Y. Fu, T. Viraraghavan, Fungal decolorization of dye wastewaters: A review, Bioresour. Technol. 79 (2001) 251–262.

[9] W.S. Alencar, E. Acayanka, E.C. Lima, B. Royer, F.E. de Souza, J. Lameira, Application of *Mangifera indica* (mango) seeds as a biosorbent for removal of Victazol Orange 3R dye from aqueous solution and study of the biosorption mechanism, Chem. Eng. J. 209 (2012) 577–588.

[10] M. Asgher, H.N. Bhatti, Evaluation of thermodynamics and effect of chemical treatments on sorption potential of Citrus waste biomass for removal of anionic dyes from aqueous solutions, Ecol. Eng. 38 (2012) 79–85.

[11] J.M. Luo, X. Xiao, S.L. Luo, Trans nonferrous, Met. Soc. China 20 (2010) 1104–1111.

[12] S.J. You, J.Y. Teng, Anaerobic decolorization bacteria for the treatment of azo dye in a sequential anaerobic and aerobic membrane bioreactor, J. Taiwan Inst. Chem. Eng. 40 (2009) 500–504.

[13] P. Kaushik, A. Malik, Fungal dye decolourization: Recent advances and future potential, Environ. Int. 35 (2009) 127–141.

[14] S. Ertuğrul, N.O. San, G. Do¨nmez, Treatment of dye (Remazol Blue) and heavy metals using yeast cells with the purpose of managing polluted textile wastewaters, Ecol. Eng. 35 (2009) 128–134.

[15] V.K. Gupta, A. Rastogi, A. Nayak, Biosorption of nickel onto treated alga (*Oedogonium hatei*): Application of isotherm and kinetic models, J. Colloid Interface Sci. 342 (2010) 533–539.

[16] A. Mittal, V.K. Gupta, A. Malviya, J. Mittal, Process development for the batch and bulk removal and recovery of a hazardous, water-soluble azo dye (Metanil Yellow) by adsorption over waste materials (Bottom Ash and De-Oiled Soya), J. Hazard. Mater. 151 (2008) 821–832.

[17] N. Kuyucak, B. Volesky, Biosorption by algal biomass, Ch.2.4 in Biosorption of heavy metals, (1990) 173–198.

[18] R.E. Lee, Phycology, Cambridge University Press, Cambridge, UK, 1989, p. 645.

[19] H.C. Bold, M.J. Wynne, Introduction to the Algae, Prentice-Hall, Englewood Cliffs, NJ, 1985, p. 516.

[20] Z.R. Holan, B. Volesky, I. Prasetyo, Biosorption of cadmium by biomass of marine algae, Biotechnol. Bioeng. 41 (1993) 819–825.

[21] R.H. Crist, J.R. Martin, D.R. Crist, Interaction of metals and protons with algae. Equilibrium constants and ionic mechanisms for heavy metal removal as sulfides and hydroxides, in: R.W. Smith, M. Misra (Eds.), Mineral Bioprocessing, The Minerals, Metals and Materials Society, Washington, DC, 1991, 275–287.

[22] J.W. Nelly, E.G. Isacoff, Carbonaceous Adsorbents for the Treatment of Ground and Surface water, Marcel Dekker, New York, NY, 1982.

[23] S. Gupta, A. Pal, P.K. Ghosh, M. Bandyopadhyay, Performance of waste activated carbon as a low-cost adsorbent for the removal of anionic surfactant from aquatic environment, J. Environ. Sci. Health, Part A 38 (2003) 381–397.

[24] A.S. Sartape, A.M. Mandhare, V.V. Jadhav, P.D. Raut, M.A. Anuse, S.S. Kolekar, Removal of Malachite green dye from aqueous solution with adsorption technique using *Limonia acidissima* (wood apple) shell as low cost adsorbent, Arab. J. Chem. (2013), in press.

[25] M.A. Al-Ghouti, M.A.M. Khraisheh, S.J. Allen, M.N. Ahmad, The removal of dyes from textile wastewater: A study of the physical characteristics and adsorption mechanisms of diatomaceous earth, J. Environ. Manage. 69 (2003) 229–238.

[26] T. Santhi, S. Manonmani, T. Smitha, Removal of malachite green from aqueous solution by activated carbon prepared from the epicarp of *Ricinus communis* by adsorption, J. Hazard. Mater. 179 (2010) 178–186.

[27] P. Saha, S. Chowdhury, S. Gupta, I. Kumar, R. Kumar, Assessment on the removal of malachite green using tamarind fruit shell as biosorbent, Clean—Soil Air Water 38 (2010) 437.
[28] R.J.P. Williams, A general introduction to the special properties of calcium ion and their development in biology, Phil. Trans. R. Soc. B. 57 (1981) 294–298.
[29] K.V. Kumar, V. Ramamurthi, S. Sivanesan, Modeling the mechanism involved during the sorption of methylene blue onto fly ash, J. Colloid Interface Sci. 284 (2005) 14–21.
[30] R. Sivaraj, C. Namasivayam, K. Kadirvelu, Orange peel as an adsorbent in the removal of Acid violet 17 (acid dye) from aqueous solutions, Waste Manage. 21 (2001) 105–110.
[31] G.C. Çetinkaya Dönmez, Z. Aksu, A. Öztürk, T.A. Kutsal, A comparative study on heavy metal biosorption characteristics of some algae, Process Biochem. 34 (1999) 885–892.
[32] Zümriye Aksu, S. Tezer, Equilibrium and kinetic modelling of biosorption of Remazol Black B by Rhizopus arrhizus in a batch system: Effect of temperature, Process Biochem. 36 (2000) 431–439.
[33] I.D. Mall, V.C. Srivastava, N.K. Agarwal, I.M. Mishra, Adsorptive removal of malachite green dye from aqueous solution by bagasse fly ash and activated carbon-kinetic study and equilibrium isotherm analyses, Colloids Surf. A: Physicochem. Eng. Aspects 264 (2005) 17–28.
[34] M.M. Abd El-Latif, A.M. Ibrahim, M.F. El-Kady, Adsorption Equilibrium, kinetics and thermodynamics of methylene blue from aqueous from aqueous solution using new activated carbons solutions using biopolymer oak sawdust composite, J. Am. Sci. 6 (2010) 267–283.
[35] J. Eastoe, J.S. Dalton, Dynamic surface tension and adsorption mechanisms of surfactants at the air water interface, Adv. Colloid Interface Sci. 85 (2000) 103–144.
[36] G. Crini, Non-conventional low-cost adsorbents for dye removal: A review, Bioresour. Technol. 97 (2006) 1061–1085.
[37] B.H. Hameed, D.K. Mahmoud, A.L. Ahmad, Sorption equilibrium and kinetics of basic dye from aqueous solution using banana stalk waste, J. Hazard. Mater. 158 (2008) 499–506.
[38] I.A.W. Tan, B.H. Hameed, A.L. Ahmad, Equilibrium and kinetic studies on basic dye adsorption by oil palm fibre activated carbon, Chem. Eng. J. 127 (2007) 111–119.
[39] R.E. Treybal, Mass Transfer Operations, second ed., McGraw Hill, New York, NY, 1968.
[40] V.J.P. Poots, G. McKay, J.J. Healy, Removal of basic dye from effluent using wood as an adsorbent, J. Water Pollut. Contr. Fed. 50 (1978) 926–935.
[41] Y.S. Ho, G. McKay, Sorption of dye from aqueous solution by peat, Chem. Eng. J. 70 (1998) 115–124.
[42] J. Singh, G. Kaur, Freundlich, Langmuir adsorption isotherms and kinetics for the removal of malachite green from aqueous solutions using agricultural waste rice straw, Int. J. Environ. Sci. 4 (2013) 250–258.
[43] R. Rajesh Kannan, M. Rajasimman, N. Rajamohan, B. Sivaprakash, Brown marine algae turbinaria conoides as biosorbent for Malachite green removal: Equilibrium and kinetic modeling, Front. Environ. Sci. Eng. China 4 (2010) 116–122.
[44] Z. Chen, H. Deng, C. Chen, Y. Yang, X. Heng, Biosorption of malachite green from aqueous solutions by *Pleurotus ostreatususing* Taguchi method, J. Environ. Health Sci. Eng. 12 (2014) 1–10.
[45] J. Zhang, Y. Li, C. Zhang, Y. Jing, Adsorption of malachite green from aqueous solution onto carbon prepared from Arundo donax root, J. Hazard. Mater. 150 (2008) 774–782.
[46] S.S. Tahir, N. Rauf, Removal of a cationic dye from aqueous solutions by adsorption onto bentonite clay, Chemosphere 63 (2006) 1842–1848.
[47] P. Saha, S. Chowdhury, S. Gupta, I. Kumar, R. Kumar, Assessment on the removal of malachite green using tamarind fruit shell as biosorbent, Clean—Soil Air Water 38 (2010) 437.
[48] P.T. Godbole, A.D. Sawant, Removal of malachite green from aqueous solutions using immobilized *Saccharomyces cerevisiae*, J. Sci. Ind. Res. 65 (2006) 440–442.
[49] C. Pradeep-Sekhar, S. Kalidhasan, V. Rajesh, N. Rajesh, Bio-polymer adsorbent for the removal of malachite green from aqueous solution, Chemosphere 77 (2009) 842–847.
[50] K.V. Kumar, S. Sivanesan, Isotherms for Malachite Green onto rubber wood (*Hevea brasiliensis*) sawdust: Comparison of linear and non-linear methods, Dyes Pigm. 72 (2007) 124–129.
[51] Y.S. Ho, G. McKay, The sorption of lead(II) ions on peat, Water Res. 33 (1999) 578–584.
[52] Y.S. Ho, G. McKay, Sorption of dye from aqueous solution by peat, Chem. Eng. J. 70 (1998) 115–124.
[53] B.H. Hameed, M.I. El-Khaiary, Malachite green adsorption by rattan sawdust: Isotherm, kinetic and mechanism modeling, J. Hazard. Mater. 159 (2008) 574–579.
[54] I.A.W. Tan, B.H. Hameed, Adsorption isotherms, kinetics, thermodynamics and desorption of activated carbon derived from oil palm empty fruit bunch, J. Appl. Sci. 10 (2010) 2565–2571.
[55] T.A. Davis, B. Volesky, A. Mucci, A review of the biochemistry of heavy metal biosorption by brown algae, Water Res. 37 (2003) 4311–4330.